Selective apoptosis of pluripotent mouse and human stem cells by novel ceramide analogues prevents teratoma formation and enriches for neural precursors in ES cell–derived neural transplants

Erhard Bieberich,[1] Jeane Silva,[1] Guanghu Wang,[1] Kannan Krishnamurthy,[1] and Brian G. Condie[1,2]

[1]Institute of Molecular Medicine and Genetics, School of Medicine, Medical College of Georgia, Augusta, GA 30912
[2]University of Georgia, Department of Genetics, University of Georgia, Athens, GA 30602

The formation of stem cell–derived tumors (teratomas) is observed when engrafting undifferentiated embryonic stem (ES) cells, embryoid body–derived cells (EBCs), or mammalian embryos and is a significant obstacle to stem cell therapy. We show that in tumors formed after engraftment of EBCs into mouse brain, expression of the pluripotency marker Oct-4 colocalized with that of prostate apoptosis response-4 (PAR-4), a protein mediating ceramide-induced apoptosis during neural differentiation of ES cells. We tested the ability of the novel ceramide analogue N-oleoyl serinol (S18) to eliminate mouse and human Oct-4(+)/PAR-4(+) cells and to increase the proportion of nestin(+) neuroprogenitors in EBC-derived cell cultures and grafts. S18-treated EBCs persisted in the hippocampal area and showed neuronal lineage differentiation as indicated by the expression of β-tubulin III. However, untreated cells formed numerous teratomas that contained derivatives of endoderm, mesoderm, and ectoderm. Our results show for the first time that ceramide-induced apoptosis eliminates residual, pluripotent EBCs, prevents teratoma formation, and enriches the EBCs for cells that undergo neural differentiation after transplantation.

Introduction

Pluripotent embryonic stem (ES) cells can be differentiated in vitro to form a wide array of cell types including germ cells and a variety of somatic cells including neurons (Deacon et al., 1998; Brustle et al., 1999; Reubinoff et al., 2001; Rossant, 2001; Bjorklund et al., 2002; Gottlieb, 2002; Barberi et al., 2003; Carpenter et al., 2003; Hubner et al., 2003). However, grafts of stem cells derived from ES cells differentiated via embryoid bodies (EBs) can be contaminated with residual pluripotent cell types leading to the formation of teratomas in the host (Bjorklund et al., 2002; Barberi et al., 2003; Erdo et al., 2003). It is only poorly understood which extra- or intracellular signals determine the lineage specification of differentiating stem cells or maintain their pluripotency, in particular in the host tissue after transplantation. In the mouse, teratomas or teratocarcinomas can be experimentally induced by transplanting early stage embryos to ectopic sites (Martin, 1980). Similarly, in transplants of cells derived from ES cells, the formation of teratomas appears to correlate with the degree to which the cells are differentiated and enriched in cell culture before grafting (Deacon et al., 1998; Bjorklund et al., 2002). The loss of teratoma forming potential is probably due to the loss of pluripotent cells that express Oct-4 (Pou5f1), an octamer-type transcription factor and a marker protein for undifferentiated, pluripotent stem cells that has also been found to be overexpressed in a variety of cancers (Monk and Holding, 2001; Pesce and Scholer, 2001; Brickman and Burdon, 2002; D'Amour and Gage, 2003). During in vitro neural differentiation of ES cells, the expression of Oct-4 is terminated and followed by up-regulation of nestin, an intermediate filament protein and marker for committed neural precursor cells (Cai et al., 2002; Pevny and Rao, 2003). This observation implies that in teratomas, the expression of Oct-4 may persist in a portion of the transplanted cells, which most likely results in their hyperproliferation and tumor formation instead of commitment to further neural differentiation. It is important to develop a greater understanding of how pluripotent cell types can persist in ES-derived cell grafts and to explore additional or alternative

Correspondence to Erhard Bieberich: ebieberich@mail.mcg.edu; or Brian G. Condie: bcondie@mail.mcg.edu

Abbreviations used in this paper: EB, embryoid body; EBC, EB-derived cell; ES; embryonic stem; FLICA, fluorochrome inhibitor of caspase; MACS, magnetic-activated cell sorting; NP, neuroprogenitor; PAR-4, prostate apoptosis response-4.

The Journal of Cell Biology, Vol. 167, No. 4, November 22, 2004 723–734
http://www.jcb.org/cgi/doi/10.1083/jcb.200405144

approaches to remove pluripotent cells from ES-derived cells. One attractive approach is to exploit the differential sensitivity to apoptosis inducers to rid neuroprogenitors (NPs) of rogue cells that are likely to form teratomas. However, there is only little known about the characteristics of tumorigenic stem cells, and there are no methods established to actively eliminate these cells from the population of committed progenitor cells and differentiated cell types that can be used for safe stem cell therapy.

Most recently, we have found that the expression of prostate apoptosis response-4 (PAR-4), an endogenous inhibitor protein of atypical PKCζ, mediates ceramide or ceramide analogue-induced apoptosis in proliferating EB-derived stem cells (Bieberich et al., 2001, 2003). The apoptotic response is specific for PAR-4(+) cells because proliferating cells with low expression of PAR-4 are less sensitive to ceramide or ceramide analogue-induced apoptosis (Bieberich et al., 2003). We also observed that in cell culture, ceramide/PAR-4–induced apoptosis is predominant during or before early neural progenitor formation from mouse EB-derived cells (EBCs; Bieberich et al., 2003). However, the majority of EBC-derived nestin(+) cells do not express PAR-4 and are thus resistant to ceramide-inducible apoptosis. From these observations, we conclude that there is a portion of proliferating, Oct-4(+)/PAR-4(+) stem cells in EBCs that can be eliminated due to apoptosis by incubation with ceramide or ceramide analogues. In the current work, we tested the ability of S18 (N-oleoyl serinol), a novel ceramide analogue that has recently been synthesized in our laboratory to induce apoptosis in mouse and human EBCs (Bieberich et al., 2000, 2002). We used multilineage teratoma formation in neonatal mouse brain as an assay to measure the level of pluripotent cells in mouse EBCs with or without incubation with S18 before engraftment into mouse brain. Our results show for the first time that Oct-4(+)/PAR-4(+) stem cells can be eliminated and nestin(+) neural precursors can be enriched in EBCs by incubation with novel ceramide analogues and that this enrichment prevents teratoma formation and promotes neural differentiation after engraftment into mouse brain.

Results

S18-induced formation of a PAR-4–PKCζ complex and inhibition of PKCζ triggers apoptosis in EBCs

We have reported that apoptosis of EBCs is induced by simultaneous elevation of endogenous ceramide and PAR-4, a protein that binds and inhibits atypical PKCζ and a variety of other proteins (Sells et al., 1994, 1997; Diaz-Meco et al., 1996; Guo et al., 1998; Bieberich et al., 2003; Gurumurthy and Rangnekar, 2004). We have also shown that overexpression or antisense knockdown of PAR-4 increases or reduces the sensitivity of differentiating ES cells toward ceramide or ceramide analogue-inducible apoptosis, respectively (Bieberich et al., 2003). However, it remained to be investigated at which differentiation stage and how ceramide-inducible apoptosis is regulated by PAR-4–mediated inhibition of PKCζ. It has been reported that C2-ceramide induces formation of a protein complex between PKCζ and PAR-4 in PC12 cells before apoptosis (Wang et al., 1999). A potential S18-induced formation of a PKCζ–PAR-4 complex in EBCs was tested using coimmunoprecipitation assays with protein from cells that were treated with or without S18. Fig. 1 A shows that no precipitated protein was found when the primary antibody was omitted, which verified the specificity of the immunoprecipitation reaction. If the same primary antibody was used for immunoprecipitation and immunoblotting, the signal was not altered by prior incubation of the stem cells with S18. This result indicated that the amount of immunoprecipitated protein was not affected by S18. However, treatment with S18 was required to coimmunoprecipitate PKCζ or PAR-4 using primary antibodies against PAR-4 or PKCζ, respectively. This observation showed that S18 induced formation of a complex between PKCζ and its inhibitor protein PAR-4.

The amount of coimmunoprecipitated PKCζ appeared to be smaller than the total amount of PKCζ, suggesting that only a portion of the complex was immunoprecipitated using the PAR-4–specific antibody. Alternatively, S18-induced binding of a portion of PKCζ to PAR-4 may be sufficient to induce apoptosis in EBCs. To test the effect of PKCζ inhibition on the induction of apoptosis, EBCs were incubated with a pseudosubstrate inhibitor peptide of PKCζ (PZI). This peptide has been shown to specifically inhibit the activity of PKCζ or its activation in a variety of cell systems (Gailly et al., 1997; Laudanna et al., 1998; Muscella et al., 2003). Fig. 1 B shows that PZI induced apoptosis at equivalent levels regardless of the time period after replating of dissociated EBs. This result suggests that inhibition of PKCζ is sufficient to induce apoptosis in EBCs at various differentiation stages. However, when EBCs were incubated with S18 and other ceramide analogues (C2-ceramide or C16-ceramide), the degree of apoptosis dropped by ∼70% within 48 h after replating of cells from dissociated EBs (Fig. 1 B). This effect was observed for spontaneous (endogenously regulated) as well as ceramide analogue-inducible apoptosis. Fig. 1 (C and D) shows that the gene and protein expression level of PAR-4 was highest at 24 h after dissociation (NP2-stage) and dropped by 80% within the first 48 h thereafter, concomitant with the decline of the degree of spontaneous or ceramide analogue-induced apoptosis. These results suggest that ceramide analogue-induced formation of an inhibitory PAR-4–PKCζ complex and thus the degree of apoptosis in differentiating ES cells is dependent on the expression level of PAR-4.

Fig. 1 C shows the gene expression level of PAR-4, nestin, and Oct-4, a transcription factor required for the maintenance of undifferentiated and pluripotent ES cells. Our results show that at the late EB and early NP stage Oct-4, PAR-4, and nestin were coexpressed in differentiating ES cultures, indicating that pluripotent (Oct-4(+)) cells and NPs (nestin(+)) coexisted at these differentiation stages. Coexistence of pluripotent stem cells and NPs was thus concomitant with the highest degree of S18-inducible apoptosis in EBs and EBCs.

Ceramide-induced apoptosis diminishes Oct-4(+)/PAR-4(+) mouse and human stem cells in EBs

Recently, we have reported that ceramide or S18 rapidly induces apoptosis in proliferating EBCs that express a high level

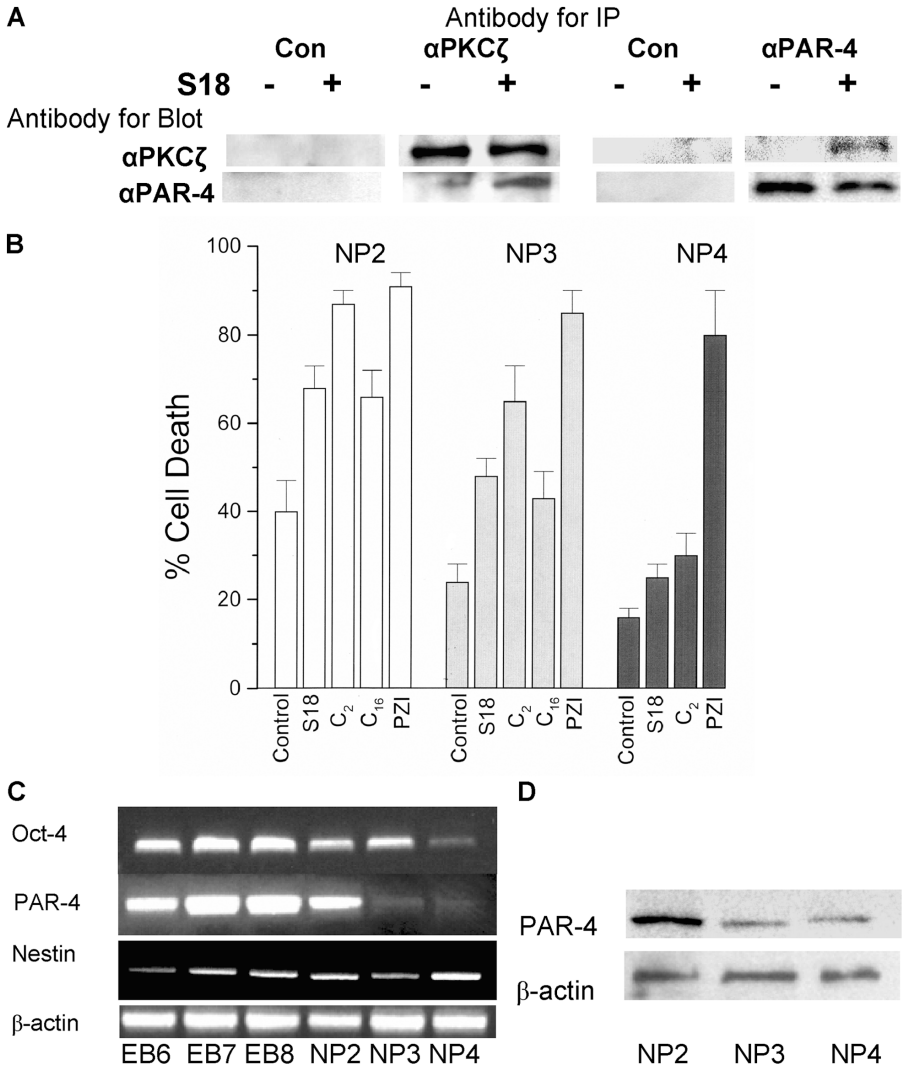

Figure 1. **S18-induced formation of a PAR-4–PKCζ complex and PAR-4 dependent apoptosis.** (A) EBCs (NP2 stage) were incubated overnight with or without 80 μM of S18. Cellular protein was solubilized and antigen–antibody complexes were immunoprecipitated, followed by SDS-PAGE and immunoblotting. (B) EBCs (NP2, 3, and 4 stages) were incubated with various ceramide-like apoptosis inducers and the degree of apoptosis was quantified by counting of cells with activated caspases (FLICA assay). All results were from three independent experiments showing average values and SEMs of cell counts from five areas with more than 100 cells. Treated cells show statistically significant differences to nontreated control cells as evaluated by ANOVA. C2, N-acetyl sphingosine (30 μM); C16, N-palmitoyl sphingosine (2 μM, incubated in solution with dodecanol as described in Bieberich et al., 2003); PZI, myristoylated PKCζ pseudosubstrate inhibitor peptide (30 μM). Open bars, NP2 stage (24 h after replating of EBCs); gray bars, NP3 stage (48 h after replating of EBCs); black bars, NP4 stage (72 h after replating of EBCs). (C and D) The level of Oct-4, PAR-4, and nestin gene expression was determined by RT-PCR during differentiation of EBCs from mouse. The expression level of PAR-4 protein was determined by immunoblotting using a mouse monoclonal anti–PAR-4 antibody. EB6, 7, and 8 are EBs 48, 72, and 96 h after attachment of suspension EBs; NP stages as in B.

of PAR-4, but little or no nestin (Bieberich et al., 2003). To determine whether or not ceramide-sensitive PAR-4(+) cells are pluripotent EBCs, we analyzed the expression of PAR-4 and Oct-4 by immunofluorescence microscopy. Fig. 2 A shows the effect of S18 on mouse EBs resulting in apoptosis and, eventually, loss of cells in the center of the EBs, whereas cells immediately surrounding the EBs were resistant toward S18. The apoptotic cells were identified as Oct-4 and PAR-4 double positive, indicating that residual Oct-4(+)/PAR-4(+) cells within the EBs maintained their sensitivity toward ceramide or ceramide analogues (Fig. 2 B). A similar subpopulation of apoptotic cells was found when EBs from human ES cells were incubated with S18 (Fig. 2 C). Confocal immunofluorescence microscopy confirmed that TUNEL(+) human cells within the EBs also stained for PAR-4 (Fig. 2 D, arrow 1) or Oct-4 and PAR-4 (Fig. 2 D, arrow 2).

To quantify the effect of ceramide-induced apoptosis on EBCs, mouse EBs cultivated in serum-free medium were incubated for 24 h with 80 μM of S18 or 2 μM of myriocin, a ceramide biosynthesis inhibitor, before magnetic-activated cell sorting (MACS) for Annexin V (+) EBCs and fluorochrome inhibitor of caspase (FLICA) tagging of activated caspases. Annexin V–MACS separated cells that were in the initial phase of apoptosis induction, whereas FLICA staining identified cells that executed apoptosis by caspase activation. Table I and Fig. 3 show the results of Oct-4 and PAR-4 staining in MACS-sorted Annexin (+) or (−) EBCs. With untreated control cells, the Annexin V(−) and (+) fractions contained PAR-4(+) and Oct-4(+) cells (Fig. 3 A), whereas with S18-treated cells, only the Annexin V(+) fraction contained PAR-4(+) and Oct-4(+) cells (Fig. 3 B). Almost all of the PAR-4(+) cells were also Oct-4(+) indicating that S18-induced apoptosis could efficiently eliminate Oct-4(+) cells from EBCs (Table I and Fig. 3 B). In cells not treated with S18, inhibition of endogenous ceramide biosynthesis with myriocin prevented apoptosis in PAR-4(+) cells, which implied that Oct-4(+) cells were preserved as well (Table I). FLICA staining revealed that S18 increased apoptosis from 25% in untreated cells to 55% in S18-treated cells, whereas <10% of the myriocin-treated cells were FLICA positive.

Within the two MACS fractions of untreated or S18-treated EBCs, more than 80% of the FLICA(+) cells were found in the Annexin V(+) fraction, which confirmed the execution of apoptosis by caspase activation and verified the

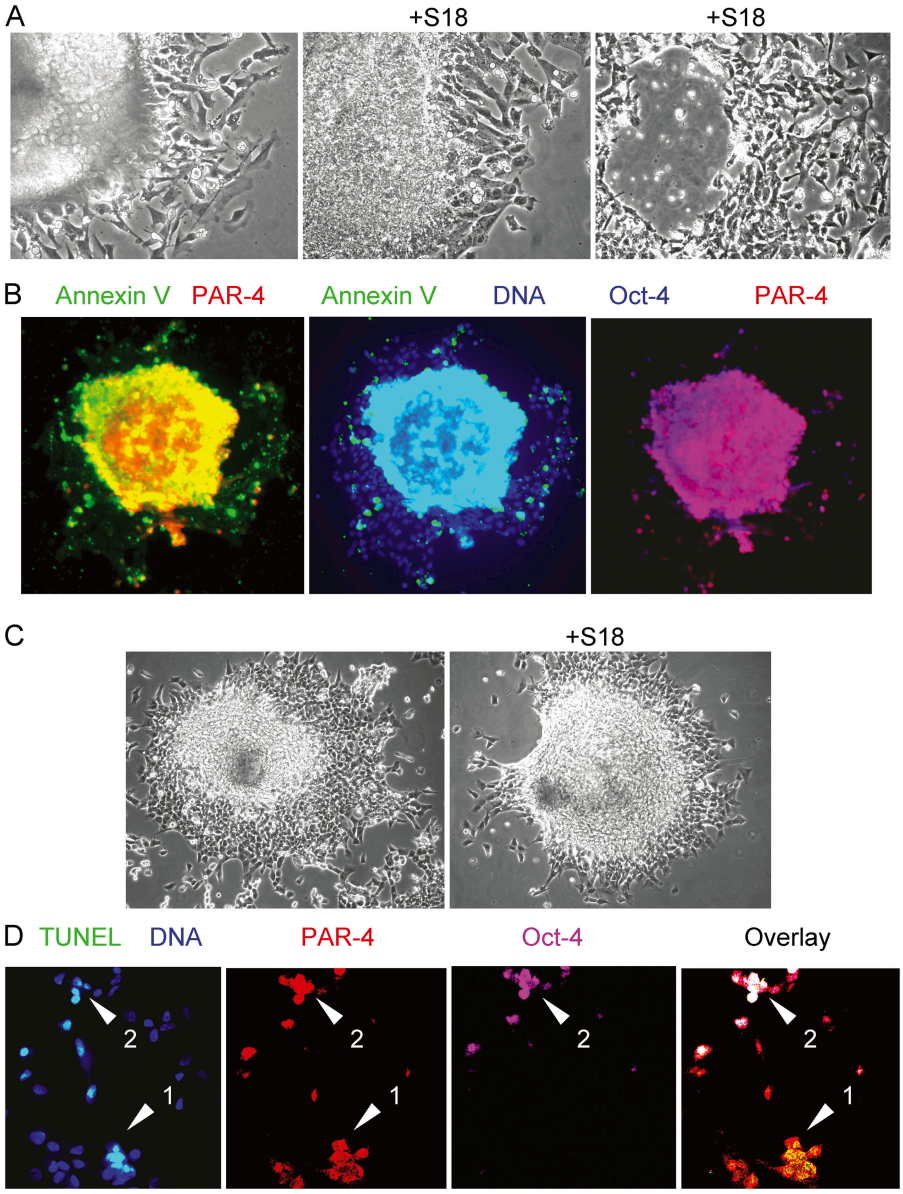

Figure 2. **Treatment with ceramide analogues eliminates Oct-4(+)/PAR-4(+) cells in EBs derived from mouse or human ES cells.** (A) Mouse EBs were incubated for 24 (middle) or 48 h (right) with 80 μM of S18 showing ongoing cell death in the peripheral and central region of the EB. (B) The center of S18-treated mouse EBs shows intensive costaining of Annexin V (FITC, green)–, PAR-4 (Cy3, red)–, and Oct-4 (Cy5, blue)–positive cells. (C and D) S18-treated human EBs were stained for apoptotic cells using TUNEL assays (FITC, green) and confocal immunofluorescence microscopy was used to detect PAR-4 (Cy3, red)– and Oct-4 (Cy5, pink)–positive cells. Arrows show apoptotic Oct-4(+)/PAR-4(+) (arrowhead 2) or Oct-4(−)/PAR-4(+) (arrowhead 1) cells.

high quality of separation by Annexin V–based MACS (Fig. 3, A and B). However, a small fraction of the Annexin V(+) cells from untreated EBs were FLICA(−) and recovered from the induction of apoptosis as indicated by their spread out morphology and noncondensed nuclei (Table I and Fig. 3 A, cells are labeled with asterisk). This population of Oct-4(+)/PAR-4(+) cells was almost completely eliminated by incubation with S18 as indicated by FLICA staining of cells in the Annexin V(+) MACS fraction (Table I and Fig. 3 B). In summary, our results show that the majority of Oct-4(+) cells also expressed PAR-4. Ceramide-induced apoptosis eliminated Oct-4(+)/PAR-4(+) cells regardless of whether ceramide was elevated by endogenous biosynthesis or was added to the medium. If apoptosis was endogenously induced, a consider-

Table I. **Expression of PAR-4 and Oct-4, and apoptosis in EBCs sorted by Annexin V–MACS**

	Annexin V negative					Annexin V positive				
	FLICA	PAR-4	Oct-4	P/O	F/P/O	FLICA	PAR-4	Oct-4	P/O	F/P/O
−S18	6 ± 1	14 ± 3	8 ± 1	8 ± 1	5 ± 2	18 ± 2	37 ± 2	26 ± 2	25 ± 1	17 ± 1
+S18	3 ± 2	5 ± 1	<2	<2	<2	48 ± 2	52 ± 3	33 ± 2	30 ± 1	28 ± 2
+Myr	2 ± 1	40 ± 3	27 ± 2	26 ± 2	<2	4 ± 1	8 ± 2	5 ± 1	5 ± 1	3 ± 1

Mouse EBs were treated as described in Fig. 2. Numbers show portion of cells with particular feature as percentage of total cells in both MACS fractions combined. Average values and SEMs were calculated from cell counts in four independent experiments with more than 100 cells in five areas used for counting. Statistical significant differences were evaluated by ANOVA. F, FLICA(+) cells; P, PAR-4(+) cells; O, Oct-4(+) cells.

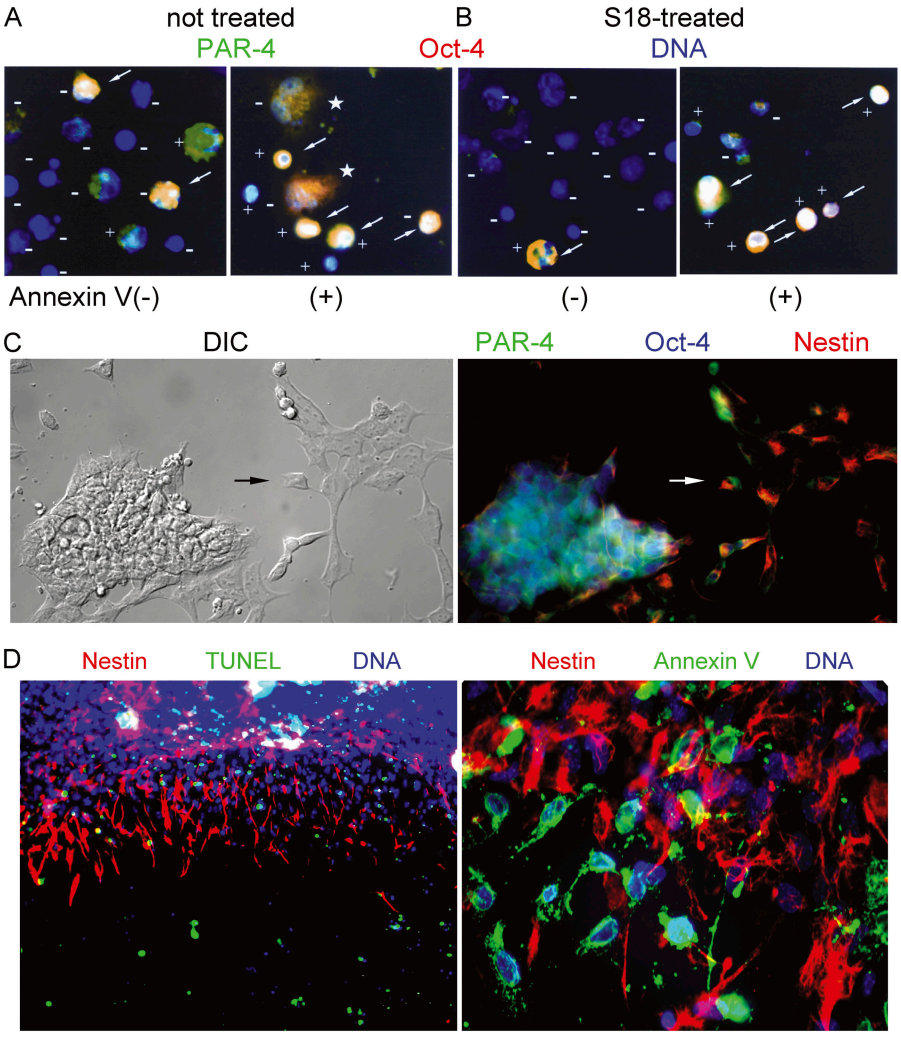

Figure 3. **S18-induced apoptosis eliminates Oct-4(+)/PAR-4(+) pluripotent stem cells and enriches for nestin(+) NPs.** (A and B) MACS sorting of apoptotic EBCs. Mouse EBCs from untreated (A) or S18-treated (80 μM; B) EBs were incubated with Annexin V–conjugated magnetic beads and fractionated using MACS. Flow through cells (Annexin V(−)) and retained cells (Annexin V(+)) were precipitated on lysine-coated coverslips, incubated with FLICA substrate, and after fixation, immunostained for the expression of PAR-4 (Cy3, red) and Oct-4 (Cy5, green). FLICA-negative and -positive cells are labeled with (−) or (+), respectively. Arrows indicate Oct-4(+)/PAR-4(+) cells. Asterisks label cells in the Annexin V(+) fraction that recovered from the initial phase of apoptosis. (C) Radial expansion and neural differentiation of mouse EBs stained for the expression of nestin (Cy3, red), PAR-4 (Cy2, green), and Oct-4 (Cy5, blue). Arrow points at cell showing coexpression and subcellular segregation of nestin and PAR-4. (D) Mouse EBs incubated overnight with 80 μM of S18 were stained for apoptotic cells (TUNEL or Annexin V, FITC, green) and nestin (Cy3, red).

able fraction of the Oct-4(+)/PAR-4(+) cells recovered from the initial phase of apoptosis induction, but was eliminated by incubation with S18.

Ceramide-induced apoptosis enriches nestin-positive neural progenitors in EBCs

We defined the population of S18-sensitive and -insensitive cells using immunocytochemistry for the expression of PAR-4, Oct-4, and nestin in attached EBs. Fig. 3 C shows that in untreated EBs, Oct-4(+)/PAR-4(+) cells are mostly confined to the center of the EBs, which is consistent with the result shown in Fig. 2 B. Nestin staining was found in cells that immediately surrounded the EB and some apparently migrating cells outside of the EBs. Consistent with our previous study (Bieberich et al., 2003), the small number of cells that coexpressed PAR-4 and nestin showed asymmetric subcellular distribution of the two proteins (Fig. 3 C, arrow). TUNEL and Annexin V staining in Fig. 3 D shows that S18 induced apoptosis selectively in nestin(−) cells of the central EB and in single, peripheral nestin(−) cells, but not in nestin(+) cells that immediately surrounded the central EB. The resistance of cells that highly express filamentous nestin toward ceramide-inducible apoptosis was also found with human EBs (unpublished data), suggesting that ceramide induces apoptosis in a similar population of pluripotent Oct-4(+)/PAR-4(+) cells derived from mouse or human EBs.

To monitor further neural differentiation of S18-treated EBCs, we determined the expression of Oct-4, PAR-4, and nestin 24 h after dissociation and replating of untreated or S18-treated EBs. Table II and Fig. 4 A show that S18 reduced the number of Oct-4(+)/PAR-4(+) by 70%, whereas the number of nestin(+) cells was not diminished. On the contrary, the portion of nestin(+) cells from S18-treated EBs showed the same proliferation rate as obtained with untreated cells and even increased by twofold (Table II), most likely due to their resistance to S18-inducible apoptosis (Bieberich et al., 2003). In contrast to untreated cells, almost all of the Oct-4(+)/PAR-4(+) cells from S18-treated EBs were FLICA(+), indicating that they were actively undergoing apoptosis and demonstrating that S18 eliminated residual Oct-4(+) positive cells from the EBCs (Table II). These results were consistent with those from MACS sorting (Table I). They also verified that S18 treatment spared the S18-resistant, nestin(+) cell population while inducing apoptosis in nearly all of the Oct-4(+) population of EBCs (Table II).

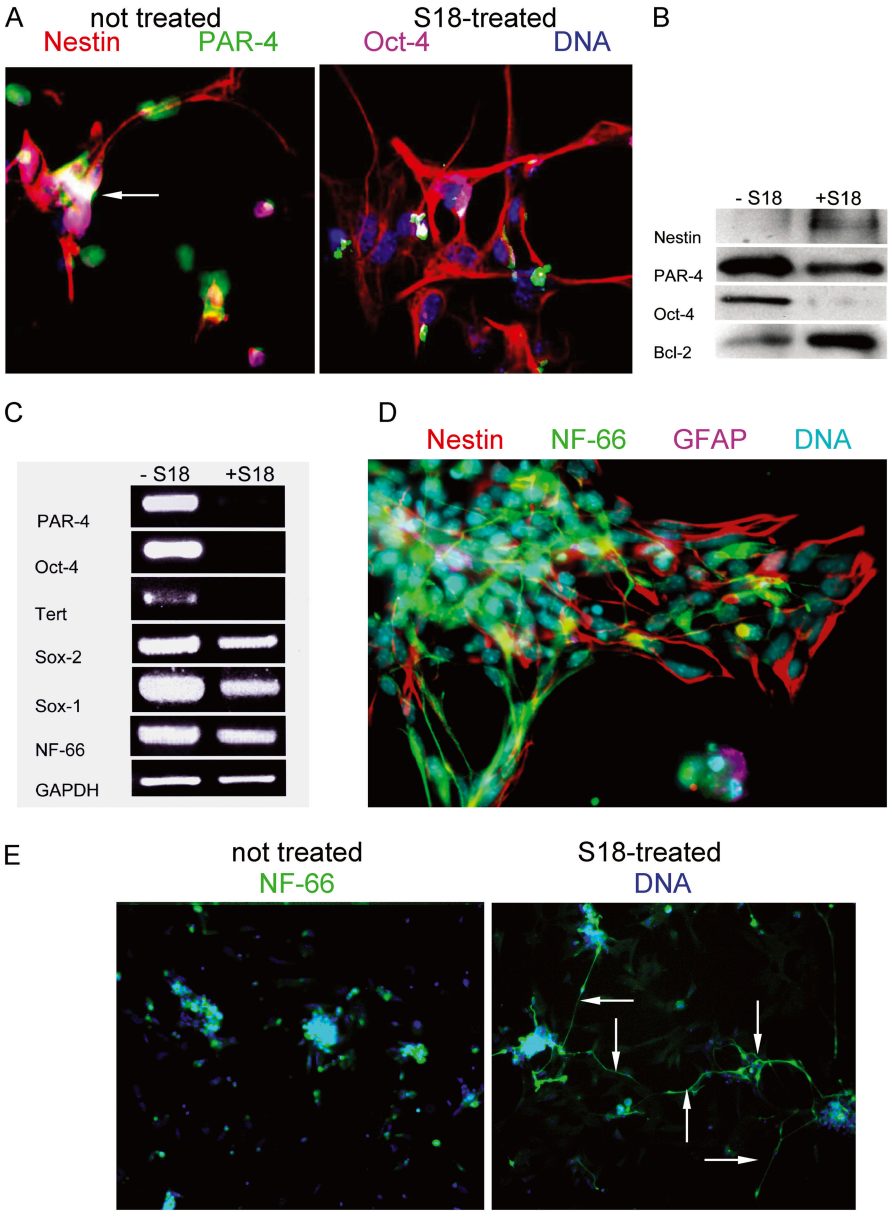

Figure 4. **Nestin(+) NPs enriched from S18-treated EBs undergo rapid neuronal differentiation.** (A) Mouse EBs were incubated with or without 80 μM of S18 and then expanded for 24 h to induce differentiation into NPs. Expanded NPs were stained for nestin (Cy3, red), PAR-4 (Cy2, green), and Oct-4 (Cy5, pink). Arrow indicates Oct-4(+)/PAR-4(+) cell. (B and C) Protein and mRNA was isolated from expanded NPs and then used for immunoblotting (B) or RT-PCR (C) for the expression of various genes and proteins (nestin, Oct-4, PAR-4, Sox-2, Sox-1, Tert, Bcl-2, and NF-66), respectively. (D) EBCs 72 h after expansion of EBs were stained for nestin (Cy3, red), NF-66 (Cy2, green), or GFAP (Cy5, pink). (E) EBCs 72 h after expansion of EBs were stained for NF-66 (Cy2, green) and DNA (Hoechst, blue). Arrows indicate cells with extensive formation of processes that stain for filamentous NF-66.

The specific enrichment of nestin(+) EBCs by S18 treatment was also shown by immunoblots indicating that the level of PAR-4 and Oct-4 protein was greatly reduced, whereas that of nestin was increased in the S18-treated cell population relative to the untreated cultures (Fig. 4 B). This observation was consistent with the diminished gene expression for Oct-4 and Tert, another marker for pluripotent stem cells, after S18 treatment (Fig. 4 C). The gene expression for Sox-2 (marker for pluripotent stem cells and NPs), Sox-1 (NP marker), and NF-66 (an early neuronal marker; Kure and Brown, 1995; Chan et al., 1997; Graham et al., 2003) was not decreased or only reduced to a limited extent, indicating that the ratio of neuronal precursor cells to pluripotent stem cells was enhanced by treatment with the ceramide analogue, which is consistent with the data shown in Table II (Bylund et al., 2003). The amount of the antiapoptotic protein Bcl-2 was increased in cells derived from S18-treated EBCs, suggesting that the subpopulation of nestin(+) cells that survived S18 treatment expressed high levels of Bcl-2, which may have protected them against S18-inducible apoptosis (Fig. 4 B).

The effect of S18 treatment on the neuronal differentiation of EBC-derived NPs was determined by immunofluorescence staining for the intermediate filament protein NF-66 and the neuronal marker MAP-2 or glial marker GFAP (Chan et al., 1997;

Table II. **Expression of PAR-4, Oct-4, and nestin, and apoptosis in expanded EBCs**

	Nestin	FLICA	PAR-4	Oct-4	PAR/Oct	F/P/O
−S18	33 ± 3	27 ± 2	55 ± 2	31 ± 2	29 ± 2	12 ± 1
+S18	64 ± 3	12 ± 1	13 ± 1	10 ± 1	9 ± 1	8 ± 1

Mouse EBs were treated and recultivated as described in Fig. 4. Numbers show portion of cells with particular feature as a percentage of total cells. For statistical evaluation see legend for Table I.

Bieberich et al., 2003). Fig. 4 D shows that NF-66 was very early expressed during NP differentiation, whereas GFAP was not expressed. In terminally differentiated cells, MAP-2(+) neurons and GFAP(+) glial cells were equally formed, which was not altered by prior incubation of EBs with S18 (unpublished data). This result indicates that S18 did not impair terminal differentiation of EBCs by eliminating Oct-4(+)/PAR-4(+) cells. On the contrary, in areas with comparable cell density, S18 treatment of EBs resulted in the early assembly of numerous NF-66(+) processes 48 h after expansion of the EBC whereas only few processes were seen without treatment (Fig. 4 E). The accelerated differentiation to NF-66(+) early neurons may have resulted from the increased population of nestin(+) NPs due to S18 treatment of EBs before expansion or may have been due to ceramide analogue-promoted neuronal differentiation.

S18-treated EBCs are less likely to form teratomas and undergo neuronal differentiation after transplantation into mouse brain

Stem cells derived from dissociated EBs are the earliest source for neural precursor cells and have been tested as a source of cells for stem cell transplantation (Deacon et al., 1998; Bjorklund et al., 2002). However, previous papers reported that in some of the animals, transplantation of EBCs resulted in the formation of stem cell–derived tumors (teratomas; Bjorklund et al., 2002; Barberi et al., 2003; Erdo et al., 2003). Because S18 treatment reduced the proportion of proliferating, pluripotent Oct-4(+)/PAR-4(+) cells in EBs, we hypothesized that S18-treated EBCs would be less likely to form teratomas in vivo. The EBCs from two ES cell lines (ES-J1 and ROSA-26) were labeled with Vybrant CM diI, a red fluorescent, nontoxic, permanent dye for tracking of the injected cells (Iwaguro et al., 2002). The injected cells were also identified by additional methods based on in situ hybridization to a fluorescent DNA probe for detection of the Y-chromosome in the male donor EBCs (Y-mapping), and by immunofluorescence staining for β-galactosidase in ROSA-26 cells (Zambrowicz et al., 1997). In each experiment, we monitored survival and neural differentiation of the EBCs by further cultivating an aliquot of the cell suspension used for injection in culture.

In preliminary studies, we found that intrastriatal injection of untreated EBCs into postnatal day 10 mice gave rise to 5–7 tumors throughout the brain after 6 wk in 12 out of 15 animals (Table III). Fig. 5 A shows a massive tumor that emerged on the surface of the right hemisphere at the injection site of the untreated EBCs. Immunohistochemistry using antibodies against α-fetoprotein, desmin, vimentin, and GFAP confirmed that the grafted EBCs had formed teratomas containing endodermal, mesodermal, and ectodermal tissues (Fig. 5 B; Vance et al., 1988; Sangruchi and Sobel, 1989). Within the teratomas, nestin expressing cells did not express PAR-4 as we would predict from previous studies of in vitro ES cell differentiation (Bieberich et al., 2003; Fig. 5 C). However, PAR-4(+)/nestin(−) cells in the center of nestin(+) cell clusters expressed Oct-4 (Fig. 5 D). These results indicated that EBC-derived teratomas maintained a subpopulation of pluripotent, Oct-4(+)/PAR-4(+)/nestin(−) stem cells.

We tested if treatment of EBs with S18 eliminated the residual pluripotent Oct-4(+)/PAR-4(+) stem cells and prevented teratoma formation from EBC-derived transplants. Table III shows that the majority of untreated ROSA-26–derived EBCs formed invasive striatal/cortical and noninvasive ventricular, β-galactosidase–positive tumors (Fig. 6 A). We labeled untreated EBCs with Vybrant CM diI (red) and S18-treated EBCs with Vybrant diO (green) and injected a mixed population of these cells into the striatum of the same mouse. Untreated, diI-labeled stem cells developed ventricular and invasive, striatal and cortical tumors, whereas S18-treated, diO-labeled cells integrated into the subependymal cell layer (Fig. 6 B and Table III) and ventromedial aspects of the hippocampus.

Fig. 6 C shows that integration of S18-treated cells in areas below the dentate gyrus was concurrent with immunostaining for nestin, indicating intensive neural precursor formation from the EBC-derived transplants. Costaining of nestin(+) neural precursors for Vybrant CM-diI, β-galactosidase, and the Y-chromosome ruled out that nestin staining was contributed by endogenous NPs, which is consistent with sparse staining of endogenous cells as reported previously (Fig. 6, C and D; Wen et al., 2002). The degree of neuronal differentiation in the nestin(+) NP layer was determined by staining for β-tubulin III, a marker for neuronal differentiation (Vance et al., 1988). Fig. 6 E shows widespread staining for β-tubulin III in S18-treated, Vybrant CM-diI–labeled EBCs used for engraftment. This result indicates that treatment of EBs with S18 prevented teratoma formation and, at the same time, allowed for neuronal differentiation after engraftment of EBCs into mouse brain.

Table III. **Tumor formation from neural transplants of EBCs from untreated and S18-treated EBs**

	Invasive tumors		Ventricular tumors	
	Animals with tumor	Tumors/animal	Animals with tumor	Tumors/animal
Untreated EBs	10/15	2 ± 1	12/15	5 ± 2
S18-treated EBs	0/15[a]	0	3/15[a]	2 ± 1

Mouse EBCs were prepared and injected into the striatum of neonatal mice (n = 15) as described in Fig. 5. Tumor formation was analyzed using coronal vibratome sections.
[a]Statistically significant differences between untreated and treated cells used for engraftment as evaluated by t test.

Discussion

We have shown that the various cell types in EBs derived from mouse and human ES cells are differentially sensitive to ceramide-inducible apoptosis. This differential sensitivity appears to be determined by whether or not the cells express the proapoptotic protein PAR-4. Our previous work had found that mouse ES cells expressing PAR-4 are rapidly induced to undergo apoptosis by the novel ceramide analogue S18 (Bieberich et al., 2001, 2003). The sensitivity of differentiating ES cells toward S18-inducible apoptosis was increased or reduced by overexpression or morpholino antisense-knockdown of PAR-4, respectively. Using Annexin V–MACS we were now able to quantify the number of PAR-4(+) EBCs in the Annexin

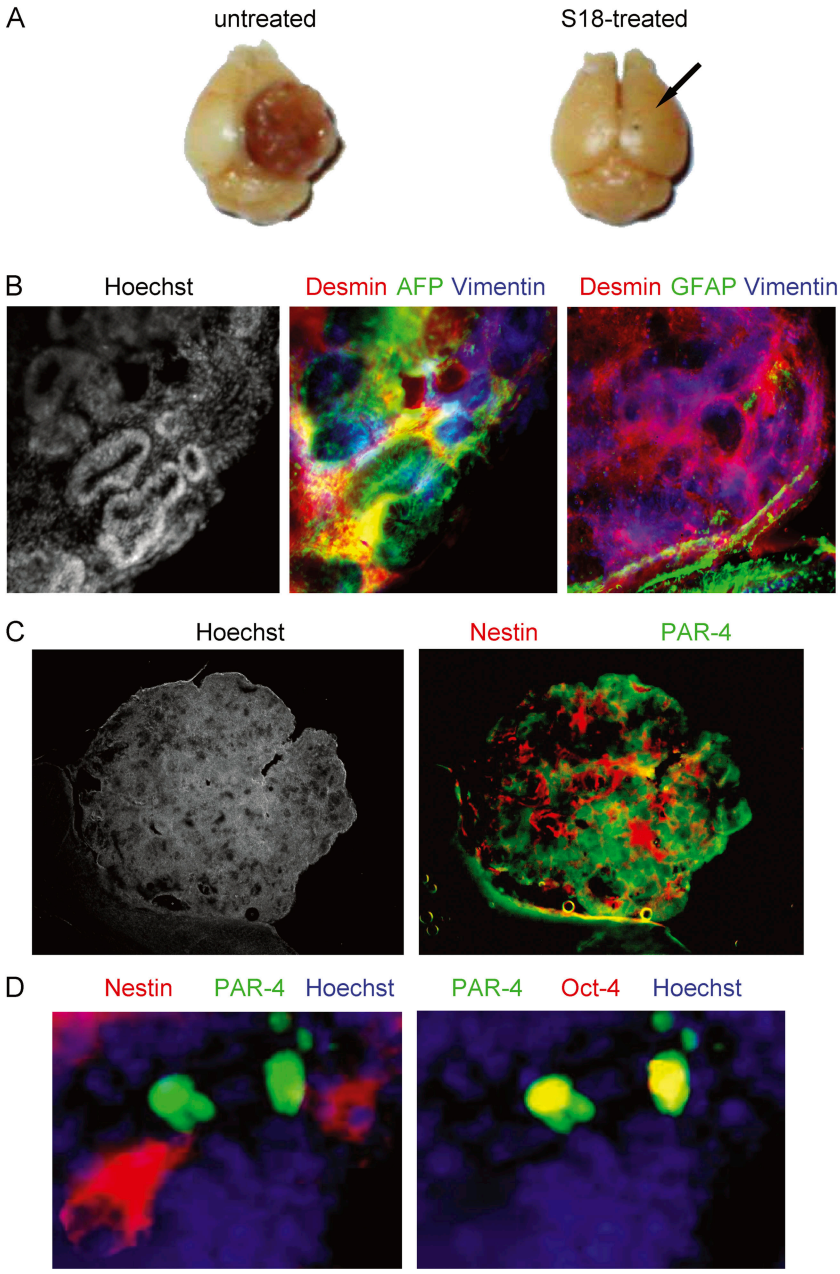

Figure 5. **Oct-4(+)/PAR-4(+) cells persist in teratomas from brain transplants of untreated EBCs.** (A) Mouse EBs were incubated with or without 80 μM of the novel ceramide analogue S18 and 100,000 untreated (left) or 200,000 S18-treated (right) EBCs injected into the striatum of C57BL6 mice (right hemisphere, arrow shows injection site). After 6 wk, mice were killed and teratoma formation was analyzed (some mice had to be killed earlier to avoid distress to the animal). (B) The teratoma obtained with untreated EBCs (left; Fig. 1 A) was vibratome sectioned and the sections immunostained for the endodermal marker α-fetoprotein (AFP, Cy2, green), the mesodermal marker desmin (Cy3, red), the ectodermal marker vimentin (Cy5, blue, middle), and the neuro-ectodermal and glial marker GFAP (Cy5, blue, right). (C) Immunohistochemistry was also performed for nestin (Cy3, red) and PAR-4 (Cy2, green). (D) Immunostaining of nestin (Cy3, red), PAR-4 (Cy2, green), and Oct-4 (Cy5, red) at higher magnification.

V(+) and (−) fractions that express the pluripotency marker Oct-4. We have shown that during mouse and human ES cell differentiation, a substantial proportion of the apoptotic and nonapoptotic Oct-4(+) EBCs also express PAR-4. Hence, we conclude that it is the high expression level of PAR-4 in the subpopulation of Oct-4(+) EBCs that confers sensitivity toward ceramide and ceramide analogues. This conclusion is also evident for other rapidly dividing cells whose sensitivity toward S18 is dependent on the expression level of PAR-4 (Bieberich et al., 2001, 2002, 2003).

Apoptosis mediated by PAR-4 may involve the regulation of several downstream targets, and inhibition of PKCζ may at least partly explain the effects observed in our paper for the following reasons: (a) the novel ceramide analogue S18 induces the formation of a protein complex between PAR-4 and PKCζ; (b) inhibition of PKCζ using a specific pseudosubstrate peptide is sufficient to induce apoptosis in EBCs; and (c) S18 eliminates the Oct-4(+)/PAR-4(+) cell population, whereas nestin(+)/PAR-4(−) cells survive, proliferate, and differentiate into neural cells. The ceramide analogue-induced elimination of Oct-4(+)/PAR-4(+) mouse and human cells suggests that a similar subpopulation of pluripotent mouse or human EBCs is specifically sensitive toward ceramide or ceramide analogues, whereas committed neural precursors are resistant. Neither the proliferation rate of nestin(+)/PAR-4(−) cells nor the ability of EBCs to undergo neuronal differentiation is diminished by the elimination of residual Oct-4(+)/PAR-4(+) EBCs. In cell transplantation experiments using EBCs, we found that teratomas contained residual nonapoptotic Oct-4(+)/PAR-4(+) cells whose specific elimination by S18-induced apoptosis before grafting prevented teratoma formation and enhanced integration of the treated cells into neural tissue.

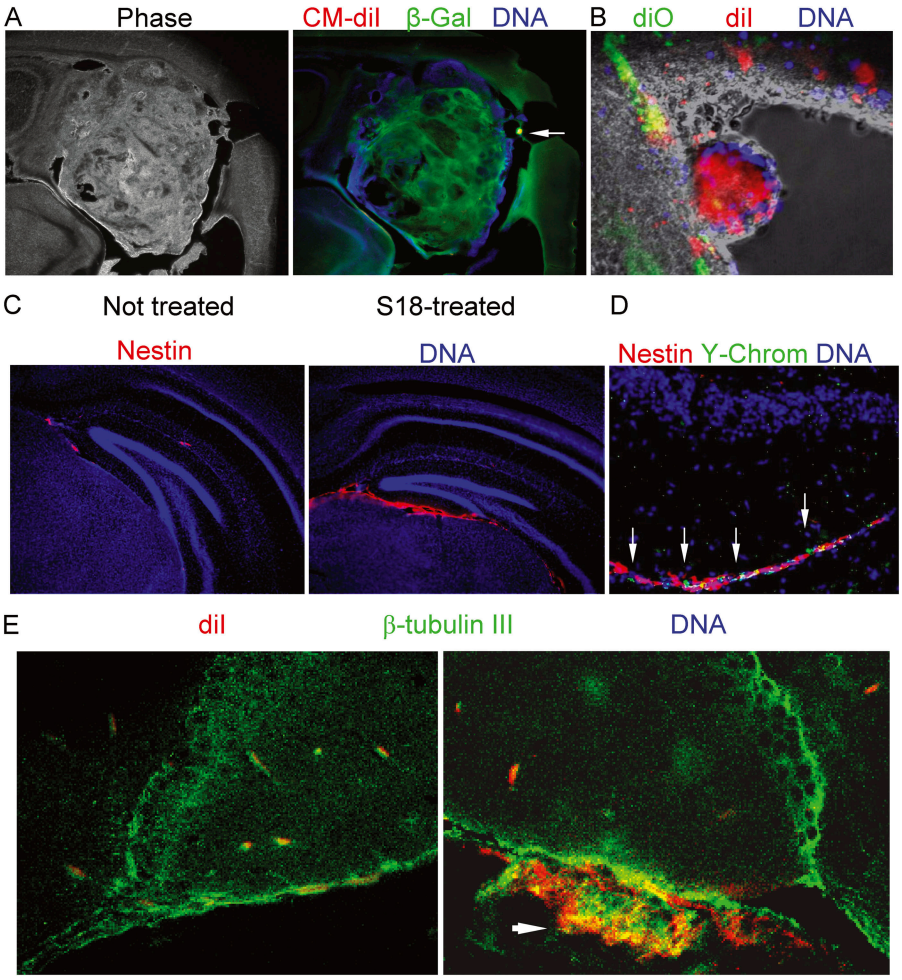

Figure 6. **EBCs from untreated EBs form highly invasive cortical and ventricular tumors, whereas S18-treated EBCs show enhanced neuronal differentiation after engraftment.** (A) A tumor developed from Vybrant CM dil-labeled ROSA-26 EBCs was immunostained for β-galactosidase (Cy2, green). The arrow indicates a residual cluster of Vybrant CM dil-labeled cells. (B) S18-treated or untreated EBCs were stained with Vybrant CM dil (red, untreated cells) or Vybrant diO (green, treated cells), mixed, and injected into the striatum of neonatal mice. The figure shows settlement of treated cells in the subependymal layer, whereas untreated EBCs form a neural tube-like tumor in the lumen of the right lateral ventricle. (C) Mouse EBCs derived from S18-treated EBs were injected into the striatum of neonatal mice and immunostained for nestin (Cy3, red). (D) After nestin staining, frozen sections were FISH-stained for Y-chromosomes (FITC, green). DNA was counterstained with Hoechst dye (blue). (E) Mouse EBs were treated with 80 μM of S18, labeled with Vybrant CM dil (red), and injected into the striatum of neonatal mice. 6 wk after engraftment, brain sections were immunostained for β-tubulin III (Cy2, green). Arrrow shows cluster of Vybrant CM dil-positive (red) cells that are double-stained for β-tubulin III (Cy2, cryosectioned, confocal).

From these results, we conclude that treatment of EBs with S18 prevents teratoma formation from residual, pluripotent EBCs in favor of neural differentiation from enriched neural precursors.

Prevention of teratoma formation resulted from the selective elimination of Oct-4(+)/PAR-4(+) cells that were either not apoptotic or had recovered from the initial phase of apoptosis in untreated EBCs. Cells escaping from death due to reversed or interrupted apoptosis ("Zombie cells") have been reported previously (Narula et al., 2001). In the case of pluripotent stem cells, they may be a source for unwanted teratoma formation unless forced to complete programmed cell death. Selective elimination of Oct-4(+)/PAR-4(+) cells is consistent with the observation that after plating of S18-treated EBCs the ratio of nestin(+) to Oct-4(+) cells was substantially increased. The surviving S18-treated EBCs underwent rapid differentiation to neuronal precursors as shown by nestin, β-tubulin III, and NF-66 staining, in vitro as well as in vivo after grafting. The S18-treated cells integrated into the subependymal layer and in areas below the dentate gyrus. The intensive staining for neuronal markers shows early differentiation of neuronal cells, suggesting that treatment with novel ceramide analogues not only prevents teratoma formation but also supports neuronal differentiation. It has been suggested that ceramide may be involved in apoptosis and differentiation depending on the context of cell signaling. In particular, the expression of the antiapoptotic protein Bcl-2 has been found to channel the ceramide response toward neuronal differentiation, whereas the expression of PAR-4 favors an apoptotic response (Diaz-Meco et al., 1996; Zhang et al., 1996; Sells et al., 1997; Guo et al., 1998; Suzuki and Tsutomi, 1998; Bieberich et al., 2000, 2003; Chen et al., 2001; Esdar et al., 2001; Luberto et al., 2002; Liang et al., 2003). These results are consistent with the observation that the expression of Bcl-2 is elevated in S18-treated EBCs that survive ceramide-induced apoptosis und undergo further neuronal differentiation.

Several investigators have performed neural cell transplants using mouse or human ES cell–derived cell types (Deacon et al., 1998; Brustle et al., 1999; Rossant, 2001; Reubinoff et al., 2001; Bjorklund et al., 2002; Gottlieb, 2002; Carpenter et al., 2003; Hubner et al., 2003). In many of these studies teratomas were not reported. In these cases, the transplanted cells were differentiated cell types that had been derived from the ES cells using lengthy multistep procedures involving repeated passaging and exposure to growth/differentiation factors or retinoic acid (Brustle et al., 1999; Reubinoff et al., 2001; Gottlieb, 2002; Barberi et al., 2003; Carpenter et al., 2003). An alternative approach has been reported for generating functional midbrain dopaminergic neurons from mouse ES cells by transplanting cells derived from EBs after only 4 d of differentiation in suspension culture. Although these investigators injected

many fewer EBCs (1–2 $\times$ 10^3 cells) compared with the number used in our injections (10^5 cells), teratomas still formed in ~26% (5/19) of the hosts and an additional 15% (3/19) contained graft-derived nonneural cell types (Bjorklund et al., 2002). Our work suggests that treatment of EBCs with ceramide or novel ceramide analogues kills pluripotent cells, enriches for neural progenitors, and obliterates the teratoma forming potential of these cells. In future work, we will investigate the regulatory interdependence of pluripotency (as determined by Oct-4) and sensitivity toward ceramide-inducible apoptosis (as determined by PAR-4). We will also graft S18-treated EBCs into adult mice and investigate if these cells survive and differentiate in a more hostile environment as present in the adult brain. Our results suggest that exposure to novel ceramide analogues may be a useful new method for eliminating pluripotent cell types from differentiating ES cell cultures before transplantation and, subsequently, enhancing neuronal differentiation for safe stem cell therapy.

Materials and methods

Materials

ES-J1 and feeder fibroblasts were purchased from the ES core facility (A. Eroglu, Medical College of Georgia, Augusta, GA). ROSA-26 cells were a gift from P. Soriano (Fred Hutchinson Cancer Research Center, Seattle, WA). The National Institutes of Health–registered human ES cell line BG01 was obtained from BresaGen and were karyotypic normal. Polyclonal rabbit antibody against NF-66 was provided by F.C.A. Chiu (Medical College of Georgia, Augusta, GA). Knockout DME, Knockout serum replacement, ES qualified FBS, N2 supplement, and FGF-2 were obtained from Invitrogen/GIBCO BRL. DME/F-12 50/50 mix was purchased from Cellgro. Nonenzymatic cell dissociation solution, Hoechst 33258, myriocin, polyclonal antivimentin goat antiserum, and goat anti–rabbit IgG HRP conjugate were obtained from Sigma-Aldrich. Myristoylated PKCζ pseudosubstrate inhibitor peptide was obtained from Calbiochem. N-acetyl sphingosine (C2-ceramide) and N-palmitoyl sphingosine (C16-ceramide) was obtained from Matreya. Polyclonal anti–Oct-4 rabbit IgG, polyclonal anti–α-fetoprotein rabbit IgG, polyclonal anti-PAR-4 rabbit IgG, polyclonal anti-PAR-4 goat IgG, and monoclonal anti-PAR-4 mouse IgG were purchased from Santa Cruz Biotechnology, Inc. Polyclonal anti-cleaved caspase 3 rabbit IgG was purchased from Cell Signaling Technologies. Anti-mouse nestin mouse monoclonal IgG (clone Rat 401), anti-desmin mouse monoclonal IgG (clone RD 301), and anti-Bcl-2 monoclonal mouse IgG (clone 7) were obtained from BD Biosciences. Polyclonal anti–β galactosidase rabbit IgG was obtained from Abcam and monoclonal anti–β galactosidase mouse IgG (clone 40-1a) was obtained from the Developmental Studies Hybridoma Bank. Donkey anti–mouse, –rabbit, and –goat IgG Cy2, Cy3, and Cy5 conjugates, goat anti–mouse IgG HRP conjugate, and normal donkey serum were purchased from Jackson ImmunoResearch Laboratories. Monoclonal anti–β tubulin III mouse IgG (clone TU-20), mouse anti–human nestin monoclonal IgG (clone 10C2), ESGRO (LIF), and the pan-caspase FLICA assay kit were obtained from Chemicon. The in situ TUNEL fluorescence staining kit was purchased from Oncogene Research Products, and the mouse chromosome Y FISH kit was obtained from Cambio. Alexa 488–conjugated Annexin V and Vybrant CM dil and diO were obtained from Molecular Probes. The MACS kit including Annexin V–conjugated magnetic beads was purchased from Miltenyi Biotec. All reagents were of analytical grade or higher and solvents were freshly redistilled before use.

Methods

ES cell differentiation, apoptosis induction, and MACS. In vitro neural differentiation of mouse and human ES cells (ES-J1, ROSA 26) followed a serum deprivation protocol as described previously (Okabe et al., 1996; Hancock et al., 2000; Bieberich et al., 2003). For MACS, cells were dissociated by incubation with trypsin, washed with PBS, and incubated for 20 min at 4°C with Annexin V–conjugated magnetic beads. Annexin V–negative (flow through) and –positive (retained cells) fractions were collected by passage through a MACS column following the manufacturer's (Miltenyi Biotec) procedures.

Transplantation of mouse EBCs. The ceramide analogue-treated or untreated mouse EBs were nonenzymatically dissociated and labeled with Vybrant CM dil or diO according to the manufacturer's protocol (Molecular Probes). The dissociated EBCs were used for in vitro neural differentiation or transplantation into the striatum of 10-d-old C57CLB6 mice by intracranial injection (bregma −1 mm, right hemisphere 2 mm off suture, 2 mm deep) of 10^5 EBCs in 5 μl of 0.9% sterile saline solution (Yanai et al., 1995). We transplanted equal numbers of viable untreated and S18-treated cells as determined by trypan blue staining.

Immunostaining, Y-FISH, and apoptosis assays. Differentiating ES cells (EBs and EBCs) on poly-L-ornithine/laminin-coated coverslips or frozen brain sections were fixed with 4% PFA in PBS and then permeabilized by incubation with 0.2% Triton X-100 in PBS for 5 min at RT. TUNEL assays were performed before immunostaining according to a protocol provided by the supplier (Oncogene Research Products). FLICA assays for active caspases were performed with living cells before fixation following the manufacturer's protocol (Chemicon). The immunostaining of fixed cells or brain sections followed procedures described previously using a blocking solution of 3% ovalbumin/2% donkey serum in PBS and concentrations of 5 μg/ml primary or secondary antibody in 0.1% ovalbumin/PBS (Bieberich et al., 2000, 2002). Y-chromosome FISH was performed according to the supplier's instructions (Cambio) after the brain sections were immunostained and underwent a second round of fixation with 4% PFA in PBS. Cell nuclei were stained with 2 μg/ml of Hoechst 33258 in PBS for 30 min at RT. Antigen specific immunostaining was quantified by counting cells that showed signals twofold or more above background fluorescence and the cell counts statistically evaluated using ANOVA and a Chi Square test as described previously (Bieberich et al., 2003). Epifluorescence microscopy was performed with a microscope (model Axiophot; Carl Zeiss MicroImaging, Inc.) using 40$\times$ (NA 1.0, oil, plan-apochromat) and 100$\times$ (NA 1.4, oil, plan-apochromat) objectives and a Spot II CCD camera. Confocal fluorescence microscopy was performed with a confocal scanning microscope (model LSM 510; Carl Zeiss MicroImaging, Inc.; equipped with Argon-488 and He-Neon 543, 633 lasers) using 40$\times$ (NA 1.3, oil, plan-neofluor) and 63$\times$ (NA 1.4, oil, apochromat) objectives. Fluorochromes are listed in Materials and methods and the legends for the figures. Spot Software (Scientific Diagnostics) and LSM 510 Meta 3.2 software (Carl Zeiss MicroImaging, Inc.) was used for image acquisition from epifluorescence or confocal microscopy, respectively. Adobe Photoshop 7.0 software was used for background reduction, pseudo-colorizing, and overlaying of pseudo-colorized grayscale images.

RT-PCR. Total RNA was prepared from ceramide analogue-treated or untreated EBCs using the Trizol method following the manufacturer's (Life Systems) protocol. PCR was performed by applying 35 cycles with various amounts of first strand cDNA template (equivalent to 0.05–0.2 μg of RNA) and 20 pmoles of sense and antisense oligonucleotide primer. The following oligonucleotide primer sequences and annealing temperatures were used: PAR-4 (sense, 5′ccagcgccaggaaaggcaaag3′; antisense, 5′ctaccttgtcagctgcccaacaac3′; 61°C), Oct-4 (sense, 5′ggagaggtgaaaccgtccctagg3′; antisense, 5′agaggaggttccctctgagttgc3′; 61°C); Tert (sense, 5′ctgcgtgtgcgtgctctggac3′; antisense, 5′gacctcagcaaacagcttgttctc, 60°C); Sox-2 (sense, 5′gtggaaacttttgtccgagac3′; antisense, 5′tggagtgggaggaaggaggtaac3′, 53°C); Sox-1 (sense, 5′ctgctcaagaaggacaagta3′; antisense, 5′ctcatgtagccctgagagt3′, 52°C); NF-66 (sense, 5′gcacgtaccattgagataga3′, antisense, 5′ctggtactttcttctgtagc3′ 52°C); GAPDH (sense, 5′gaaggtgaaggtcggagtcaacg3′; antisense, 5′ggtgatgggatttccattgatgacaagc3′; 58°C). The amount of template from each sample was adjusted until PCR yielded equal intensities of amplification product using GAPDH-specific primers.

Miscellaneous. The amount of protein was determined following a modified Folin phenol reagent (Lowry) assay as described previously (Wang and Smith, 1975). Protein extracted with detergent was precipitated according to the Wessel and Flugge method (Wessel and Flugge, 1984). SDS-PAGE was performed using the Laemmli method followed by immunoblotting as described previously (Laemmli, 1970). Coimmunoprecipitation assays were performed as described previously (Wang et al., 1999).

We would like to thank Dr. Nancy Manley for critically reading the manuscript and Dr. Mahendra Rao for providing us with the sequences of oligonucleotide primers used for RT-PCR of differentiation markers. We thank Dr. Thomas Schulz (BresaGen, Athens, GA) for his advice on the cultivation of human stem cells. We are grateful to Drs. Paul McNeil and Katsuya Miyake (Cell Imaging Core Facility, Institute of Molecular Medicine and Genetics, Medical College of Georgia) for their help with fluorescence microscopy and image acquisition. We also thank Dr. Robert K. Yu (Institute of Molecular Medicine and Genetics, Medical College of Georgia) for continuing institutional support.

This study was funded by National Institutes of Health grants R01MH064794 to B.G. Condie and R01NS046835 to E. Bieberich.

Submitted: 24 May 2004
Accepted: 13 October 2004

References

Barberi, T., P. Klivenyi, N.Y. Calingasan, H. Lee, H. Kawamata, K. Loonam, A.L. Perrier, J. Bruses, M.E. Rubio, N. Topf, et al. 2003. Neural subtype specification of fertilization and nuclear transfer embryonic stem cells and application in parkinsonian mice. *Nat. Biotechnol.* 21:1200–1207.

Bieberich, E., T. Kawaguchi, and R.K. Yu. 2000. N-acylated serinol is a novel ceramide mimic inducing apoptosis in neuroblastoma cells. *J. Biol. Chem.* 275:177–181.

Bieberich, E., S. MacKinnon, J. Silva, and R.K. Yu. 2001. Regulation of apoptosis during neuronal differentiation by ceramide and b-series complex gangliosides. *J. Biol. Chem.* 276:44396–44404.

Bieberich, E., B. Hu, J. Silva, S. MacKinnon, R.K. Yu, H. Fillmore, W.C. Broaddus, and R.M. Ottenbrite. 2002. Synthesis and characterization of novel ceramide analogs for induction of apoptosis in human cancer cells. *Cancer Lett.* 181:55–64.

Bieberich, E., S. MacKinnon, J. Silva, S. Noggle, and B.G. Condie. 2003. Regulation of cell death in mitotic neural progenitor cells by asymmetric distribution of prostate apoptosis response 4 (PAR-4) and simultaneous elevation of endogenous ceramide. *J. Cell Biol.* 162:469–479.

Bjorklund, L.M., R. Sanchez-Pernaute, S. Chung, T. Andersson, I.Y. Chen, K.S. McNaught, A.L. Brownell, B.G. Jenkins, C. Wahlestedt, K.S. Kim, and O. Isacson. 2002. Embryonic stem cells develop into functional dopaminergic neurons after transplantation in a Parkinson rat model. *Proc. Natl. Acad. Sci. USA*. 99:2344–2349.

Brickman, J.M., and T.G. Burdon. 2002. Pluripotency and tumorigenicity. *Nat. Genet.* 32:557–558.

Brustle, O., K.N. Jones, R.D. Learish, K. Karram, K. Choudhary, O.D. Wiestler, I.D. Duncan, and R.D. McKay. 1999. Embryonic stem cell-derived glial precursors: a source of myelinating transplants. *Science.* 285:754–756.

Bylund, M., E. Andersson, B.G. Novitch, and J. Muhr. 2003. Vertebrate neurogenesis is counteracted by Sox1-3 activity. *Nat. Neurosci.* 6:1162–1168.

Cai, J., Y. Wu, T. Mirua, J.L. Pierce, M.T. Lucero, K.H. Albertine, G.J. Spangrude, and M.S. Rao. 2002. Properties of a fetal multipotent neural stem cell (NEP cell). *Dev. Biol.* 251:221–240.

Carpenter, M.K., E. Rosler, and M.S. Rao. 2003. Characterization and differentiation of human embryonic stem cells. *Cloning Stem Cells.* 5:79–88.

Chan, S.-O., D. Peng, and F.-C. Chiu. 1997. Heterogeneous expression of neurofilament proteins in forebrain and cerebellum during development: clinical implications for spinocerebellar ataxia. *Brain Res.* 775:107–118.

Chen, Y., I. Ginis, and J.M. Hallenbeck. 2001. The protective effect of ceramide in immature rat brain hypoxia-ischemia involves up-regulation of Bcl-2 and reduction of TUNEL-positive cells. *J. Cereb. Blood Flow Metab.* 21: 34–40.

Deacon, T., J. Dinsmore, L.C. Costantini, J. Ratliff, and O. Isacson. 1998. Blastula-stage stem cells can differentiate into dopaminergic and serotonergic neurons after transplantation. *Exp. Neurol.* 149:28–41.

D'Amour, K.A., and F.H. Gage. 2003. Genetic and functional differences between multipotent neural and pluripotent embryonic stem cells. *Proc. Natl. Acad. Sci. USA*. 100:11866–11872.

Diaz-Meco, M.T., M.M. Municio, S. Frutos, P. Sanchez, J. Lozano, L. Sanz, and J. Moscat. 1996. The product of par-4, a gene induced during apoptosis, interacts selectively with the atypical isoforms of protein kinase C. *Cell.* 86:777–786.

Erdo, F., C. Buhrle, J. Blunk, M. Hoehn, Y. Xia, B. Fleischmann, M. Focking, E. Kustermann, E. Kolossov, J. Hescheler, et al. 2003. Host-dependent tumorigenesis of embryonic stem cell transplantation in experimental stroke. *J. Cereb. Blood Flow Metab.* 23:780–785.

Esdar, C., S. Milasta, A. Maelicke, and T. Herget. 2001. Differentiation-associated apoptosis of neural stem cells is affected by Bcl-2 overexpression: impact on cell lineage determination. *Eur. J. Cell Biol.* 80:539–553.

Gailly, P., M.C. Gong, A.V. Somlyo, and A.P. Somlyo. 1997. Possible role of atypical protein kinase C activated by arachidonic acid in Ca^{2+} sensitization of rabbit smooth muscle. *J. Physiol.* 500:95–109.

Gottlieb, D.I. 2002. Large-scale sources of neural stem cells. *Annu. Rev. Neurosci.* 25:381–407.

Graham, V., J. Khudyakov, P. Ellis, and L. Pevny. 2003. SOX2 functions to maintain neural progenitor identity. *Neuron.* 39:749–765.

Guo, Q., W. Fu, J. Xie, H. Luo, S.F. Sells, J.W. Geddes, V. Bondada, V.M. Rangnekar, and M.P. Mattson. 1998. Par-4 is a mediator of neuronal degeneration associated with the pathogenesis of Alzheimer disease. *Nat. Med.* 4:957–962.

Gurumurthy, S., and V.M. Rangnekar. 2004. Par-4 inducible apoptosis in prostate cancer cells. *J. Cell. Biochem.* 91:504–512.

Hancock, C.R., J.P. Wetherington, N.A. Lambert, and B. Condie. 2000. Neuronal differentiation of cryopreserved neural progenitor cell derived from mouse embryonic stem cells. *Biochem. Biophys. Res. Commun.* 271: 418–421.

Hubner, K., K. Fuhrmann, L.K. Christenson, J. Kehler, R. Reinbold, R. De La Fuente, J. Wood, J.F. Strauss III, M. Boiani, and H.R. Scholer. 2003. Derivation of oocytes from mouse embryonic stem cells. *Science.* 300: 1251–1256.

Iwaguro, H., J. Yamaguchi, C. Kalka, S. Murasawa, H. Masuda, S. Hayashi, M. Silver, T. Li, J.M. Isner, and T. Asahara. 2002. Endothelial progenitor cell vascular endothelial growth factor gene transfer for vascular regeneration. *Circulation.* 105:732–738.

Kure, R., and I.R. Brown. 1995. Expression of low-molecular-weight neurofilament (NF-L) mRNA during postnatal development of the mouse brain. *Neurochem. Res.* 20:833–846.

Laemmli, U.K. 1970. Cleavage of structural proteins during the assembly of the head of bacteriophage 4. *Nature.* 227:680–685.

Laudanna, C., D. Mochly-Rosen, T. Liron, G. Constantin, and E.C. Butcher. 1998. Evidence of ζ protein kinase C involvement in polymorphonuclear neutrophil integrin-dependent adhesion and chemotaxis. *J. Biol. Chem.* 273:30306–30315.

Liang, Y., Z.K. Mirnics, C. Yan, K.D. Nylandaer, and N.F. Schor. 2003. Bcl-2 mediates induction of neural differentiation. *Oncogene.* 22:5515–5518.

Luberto, C., J.M. Kraveka, and Y.A. Hannun. 2002. Ceramide regulation of apoptosis versus differentiation: a walk on a fine line. Lessons from neurobiology. *Neurochem. Res.* 27:609–617.

Martin, G.R. 1980. Teratocarcinomas and mammalian embryogenesis. *Science.* 209:768–776.

Monk, M., and C. Holding. 2001. Human embryonic genes re-expressed in cancer cells. *Oncogene.* 20:8085–8091.

Muscella, A., S. Greco, M.G. Elia, C. Storelli, and S. Marsigliante. 2003. PKC-ζ is required for angiotensin II-induced activation of ERK and synthesis of c-fos in MCF-7 cells. *J. Cell. Physiol.* 197:61–68.

Narula, J., E. Arbustini, Y. Chandrashekhar, and M. Schwaiger. 2001. Apoptosis and the systolic dysfunction in congestive heart failure. Story of apoptosis interruptus and zombie myocytes. *Cardiol. Clin.* 19:113–126.

Okabe, S., K. Forsberg-Nilsson, A.C. Spiro, M. Segal, and R.D. McKay. 1996. Development of neuronal precursor cells and functional postmitotic neurons from embryonic stem cells in vitro. *Mech. Dev.* 59:89–102.

Pesce, M., and H.R. Scholer. 2001. Oct-4: Gatekeeper in the beginnings of mammalian development. *Stem Cells.* 19:271–278.

Pevny, L., and M.S. Rao. 2003. The stem-cell menagerie. *Trends Neurosci.* 26: 351–359.

Reubinoff, B.E., P. Itsykson, T. Turetsky, M.F. Pera, E. Reinhartz, A. Itzik, and T. Ben-Hur. 2001. Neural progenitors from human embryonic stem cells. *Nat. Biotechnol.* 19:1134–1140.

Rossant, J. 2001. Stem cells from the mammalian blastocyst. *Stem Cells.* 19: 477–482.

Sangruchi, T., and R.A. Sobel. 1989. Microglial and neural differentiation in human teratomas. *Acta Neuropathol. (Berl.).* 78:258–263.

Sells, S.F., D.P. Wood Jr., S.S. Joshi-Barve, S. Muthukumar, R.J. Jacob, S.A. Crist, S. Humphreys, and V.M. Rangnekar. 1994. Commonality of the gene programs induced by effectors of apoptosis in androgen-dependent and -independent prostate cells. *Cell Growth Differ.* 5:457–466.

Sells, S.F., S.S. Han, S. Muthukumar, N. Maddiwar, R. Johnstone, E. Boghaert, D. Gillis, G. Liu, P. Nair, S. Monnig, et al. 1997. Expression and function of the leucine zipper protein PAR-4 in apoptosis. *Mol. Cell. Biol.* 17: 3823–3832.

Suzuki, A., and Y. Tsutomi. 1998. Bcl-2 accelerates the neuronal differentiation: new evidence approaching to the biofunction of Bcl-2 in the nervous system. *Brain Res.* 801:59–66.

Vance, R.P., K.R. Geisinger, M.B. Randall, and R.B. Marshall. 1988. Immature neural elements in immature teratomas. An immunohistochemical and ultrastructural study. *Am. J. Clin. Pathol.* 90:397–411.

Wang, C.-S., and R.L. Smith. 1975. Lowry determination of protein in the presence of Triton X-100. *Anal. Biochem.* 63:414–417.

Wang, Y.M., M.L. Seibenhener, M.L. Vandenplas, and M.W. Wooten. 1999. Atypical PKCzeta is activated by ceramide, resulting in coactivation of NF-kappaB/JNK kinase and cell survival. *J. Neurosci. Res.* 55:293–302.

Wen, P.H., V.L. Friedrich Jr., J., Shioi, N.K. Robakis, and G.A. Elder. 2002. Presenilin-1 is expressed in neural progenitor cell in the hippocampus of adult mice. *Neurosci. Lett.* 318:53–56.

Wessel, D., and U.I. Flugge. 1984. A method for the quantitative recovery of protein in dilute solution in the presence of detergents and lipids. *Anal. Biochem.* 138:141–143.

Yanai, J., T. Doetchman, N. Laufer, J. Maslaton, S. Mor-Yosef, A. Safran, M. Shani, and D. Sofer. 1995. Embryonic cultures but not embryos transplanted to the mouse's brain grow rapidly without immunosuppression. *Int. J. Neurosci.* 81:21–26.

Zambrowicz, B.P., A. Imamoto, S. Fiering, L.A. Herzenberg, W.G. Kerr, and P. Soriano. 1997. Disruption of overlapping transcripts in the ROSA beta geo 26 gene trap strain leads to widespread expression of beta-galactosidase in mouse embryos and hematopoietic cells. *Proc. Natl. Acad. Sci. USA.* 94:3789–3794.

Zhang, K.-Z., J.A. Westberg, E. Holtta, and L.C. Andersson. 1996. Bcl2 regulates neural diffentiation. *Proc. Natl. Acad. Sci. USA.* 93:4504–4508.